Molecular Crystals and Liquid Crystals
Publication details, including instructions for authors and subscription information:
http://www.tandfonline.com/loi/gmcl16

# Triplet Spin Excitons in a Sigma-Bonded TCNQ Dimer Salt: N-Ethylphenazinium TCNQ, $(NEP^{+})_2$ $(TCNQ^{-}\text{-}TCNQ^{-})$

Ralf H. Harms [a], Heimo J. Keller [a], Dietrich Nöthe [a], Manfred Werner [a], Dieter Gundel [b], Hans Sixl [b], ZoltÁN G. Soos [c] & Robert M. Metzger [d]

[a] Anorganisch-Chemisches Institut, Universität Heidelberg, Im Neuenheimer Feld 270, D-6900 Heidelberg 1, Germany.

[b] Physikalisches Institut, Teil 3, Universität Stuttgart, D-7000 Stuttgart 80, Germany.

[c] Department of Chemistry, Princeton University Princeton, N.J., 08540, U.S.A.

[d] Department of Chemistry, University of Mississippi, University Miss., 38677, U.S.A.

Version of record first published: 20 Apr 2011.

*Mol. Cryst. Liq. Cryst.*, 1981, Vol. 65, pp. 179–196
0026-8941/81/6504-0179$06.50/0

Printed in the U.S.A.



# Triplet Spin Excitons in a Sigma-Bonded TCNQ Dimer Salt: N-Ethylphenazinium TCNQ, $(NEP^+)_2(TCNQ^- - TCNQ^-)$

RALF H. HARMS, HEIMO J. KELLER, DIETRICH NÖTHE, and MANFRED WERNER

*Anorganisch-Chemisches Institut, Universität Heidelberg, Im Neuenheimer Feld 270, D-6900 Heidelberg 1, Germany.*

and

DIETER GUNDEL and HANS SIXL

*Physikalisches Institut, Teil 3, Universität Stuttgart, D-7000 Stuttgart 80, Germany.*

and

ZOLTÁN G. SOOS

*Department of Chemistry, Princeton University, Princeton, N.J. 08540, U.S.A.*

and

ROBERT M. METZGER

*Department of Chemistry, University of Mississippi, University, Miss. 38677, U.S.A.*

(*Received August 7, 1980*)

The title compound NEP-TCNQ crystallizes with $\theta$-bonded ($TCNQ^-$-$TCNQ^-$)-dimers. We show by model calculations and ESR spectroscopy, that these bonds can be broken by thermal activation. The reverse reaction occurs spontaneously. The excited states are characterized as quasi immobilized triplet spin excitons (TSE) localized on the two "parts" of the former TCNQ-dimer. Additional weaker TSE and doublet signals are observed.

## 1 INTRODUCTION

We report the electron paramagnetic resonance (EPR) study of triplet spin excitons (TSE) in an ionic crystal containing $\sigma$-bonded $TCNQ^-$ dimers, $(NEP^+)_2(TCNQ^-\text{–}TCNQ^-)$, where $NEP^+$ is the diamagnetic cation 5-Ethylphenasinium, or *N*-Ethylphenazinium, and TCNQ is the potent electron acceptor 7,7,8,8-Tetracyanoquinodimethane (TCNQ).

Since the first synthesis of TCNQ in 1960,[1] TCNQ complexes have received widespread attention and thorough-going investigation[2] because of their unusual anisotropic optical and transport properties. TSE have been known in TCNQ salts since 1961[3]: these are thermal $S = 1$ excitations with orientation-dependent fine-structure splittings of the EPR signal, which occur in an underlying diamagnetic lattice of $\pi$-$\pi$ overlapping $TCNQ^-$ ($S = 1/2$) radical anions; their EPR spectrum exhibits extreme line narrowing, and only residual hyperfine effects on the exciton signal linewidth, because of the fast diffusional or hopping nature of the paramagnetic excitation, which is most pronounced along the linear chain of $TCNQ^-$ anions.[3] This behaviour is not limited to TCNQ salts.[4]

In polar solvents $TCNQ^-$ radicals can form an $S = 0$ dimerized complex with an enthalpy of formation of $-44$ kJ/mole of dimer (or 0.46 eV), which has been usually described as a $\pi$-$\pi$ complex.[5]

In the solid state most TCNQ crystals[2h] can form segregated linear stacks of $TCNQ^-$ anions ($\pi$-$\pi$ overlap), sometimes interspersed with neutral TCNQ° molecules, and sometimes mixed-valent $TCNQ^{-\gamma}$ units, such as in the quasi-one-dimensional metal TTF-TCNQ. In other cases, mixed-stack charge-transfer (CT) solids are formed, as in TMPD-TCNQ, where TMPD is *N*,*N*,*N*′,*N*′-Tetramethyl-*p*-phenylenediamine. There is $\pi$-$\pi$ overlap between the partly ionic[6] $TCNQ^{-\gamma}$ and its $S = 1/2$ counterion $TMPD^{+\gamma}$. Mixed stacking is generally found in neutral complexes with weaker donors.

In two recently reported crystal structures, however, a rather long aliphatic sigma bond has formed between two neighboring $TCNQ^-$ anions in the crystal: in $[bis(2,2'\text{-dipyridyl})platinum(II)]^{2+}$ $(TCNQ^-\text{–}TCNQ^-)$,[7] this bond is 1.65(2) Å long, and in $(NEP^+)_2(TCNQ^-\text{–}TCNQ^-)$ it is 1.631(1) Å long.[8] Such unusually long sigma bonds have been observed also in other systems.[9,10]

We have undertaken an EPR study of $(NEP^+)_2$ $(TCNQ^-\text{-}TCNQ^-)$ as part of a larger study[11] of several *N*-alkylphenazinium(NRP)-TCNQ and *N*-alkylphenazinium-$TCNQF_4$ salts, $(NRP)_2(TCNQX_4)_2$, where: $R = CH_3$, $C_2H_5$, $n$-$C_3H_7$, $n$-$C_4H_9$ and $X$ = H, F.

As discussed below, the crystals of $(NEP^+)_2$ $(TCNQ^-\text{–}TCNQ^-)$ exhibit four different EPR signals:

a) Thermally activated TSE lines which show an orientation-dependent fine structure splitting that can be identified with an $S = 1$ excitation of the

$TCNQ^-$–$TCNQ^-$ dianion, and assigned to a transition to an excited state where the long sigma bond is "broken." This excitation shows no hyperfine structure.

b) Other smaller $S = 1$ signals with much smaller fine structure splittings and nearly Curie behaviour.

c) An $S = 1/2$ "impurity" line. (Curie behaviour).

d) A narrow, thermally activated $S = 1/2$ line.

The crystal structure (Figure 1) shows that there is $\pi$-$\pi$ overlap not between adjacent $TCNQ^-$–$TCNQ^-$ dianions, but rather between one $NEP^+$ cation and the two $TCNQ^-$ "half molecules" belonging to different dianions between which the $NEP^+$ is sandwiched. Accordingly, the usual explanation of the mobility of the TSE along the stacking direction by hopping between $\pi$-$\pi$ overlapping sites in a linear chain does not apply here. We shall instead propose that "quasi-immobilized TSE" exist in $(NEP^+)_2(TCNQ^-$–$TCNQ^-)$.

In Section 2 we present and discuss the TSE signals; in Section 3 we show the behaviour of the $S = 1/2$ signals at $g = 2$. In Section 4 we discuss the solid-state implications of our results.

## 2 TRIPLET SPIN EXCITON SPECTRA

### 2.1 Crystal preparation, habit, structure, and conductivity

Crystals of $(NEP^+)_2(TCNQ^-$–$TCNQ^-)$ were grown by mixing hot solutions of $NEP^+ClO_4^-$ (1 mmol) in 60 ml absolute acetonitrile and LiTCNQ (1 mmol) in 30 ml absolute ethanol and slowly cooling to room temperature.[12] A specimen suitable for EPR analysis was selected, of size 2 mm by 1 mm by 1 mm. Its growth habit was checked by X-ray oscillation and Weissenberg photographs and by optical microscopy, and the face indices and crystal axes are identified in Figure 2. Also defined in Figure 2 is a convenient orthogonal coordinate system $[(X, Y, Z)$: $Y \| b$, $Z \| c^*$ and $X \perp Y, Z]$. The $X$-axis is 5.76 degrees from the crystallographic **a** axis (the stack axis) and 90.0 degrees from the **b** axis. The $Y$ axis coincides with the crystallographic **b** axis. The $Z$ axis coincides with the **c*** axis and is 4.36 degrees from the **c** axis. Figure 1 reproduces the projections along [1, 0, 0] and [0, 1, 0] of the published crystal structure:[8] the $TCNQ^-$–$TCNQ^-$ atoms are marked by solid circles. Figure 2 also shows the inferred orientation of the $TCNQ^-$–$TCNQ^-$ dianions inside the specimen.

Table I contains, in the orthogonal coordinate system of Figure 2, the direction angles of the normals to the least squares planes of the $NEP^+$ ion

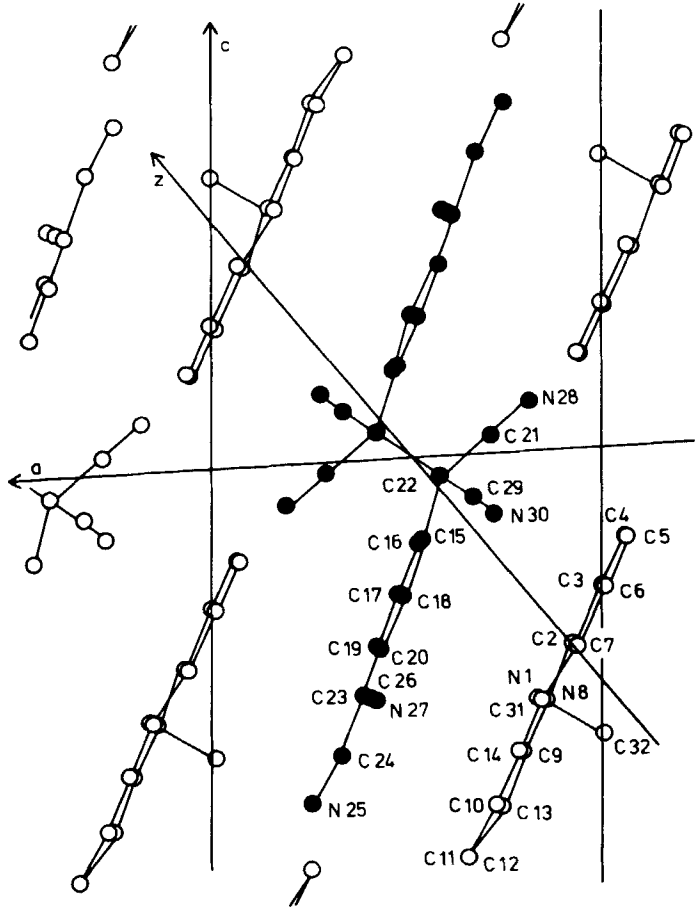


FIGURE 1 Projection of the $(NEP^+)_2(TCNQ^-\text{–}TCNQ^-)$ structure and the principal axes ($x$, $y$, $z$) of the fine structure tensor along [0, 1, 0] (Figure 1a) and [1, 0, 0] (Figure 1b) from Ref. 8. For clarity the central $TCNQ^-\text{–}TCNQ^-$ atoms are given as solid circles.

TABLE I

Direction angles $\alpha_X$, $\alpha_Y$, $\alpha_Z$ (degrees) of the relevant molecular parts of the crystal structure of $(NEP^+)_2(TCNQ^-\text{-}TCNQ^-)$ (Ref. 8) with respect to the cartesian coordinate axes $X$, $Y$, $Z$ respectively, of Figure 2

| | $\alpha_X$ | $\alpha_Y$ | $\alpha_Z$ |
|---|---|---|---|
| Normal to least-squares plane of either six-membered ring of TCNQ-TCNQ dianion | 24.37 | 91.69 | 65.70 |
| Normal to least-squares plane of all conjugated ring atoms of NEP cation | 27.86 | 91.31 | 62.17 |
| Vector C22′ to C22 (long sigma bond) | 40.00 | 78.25 | 52.44 |

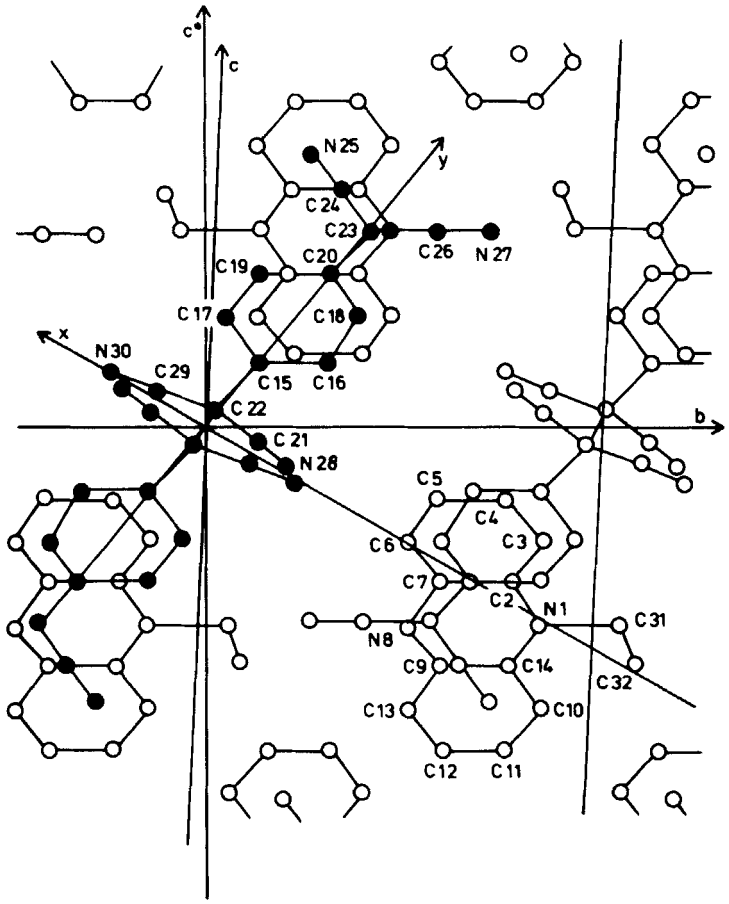


FIGURE 1b

and of the TCNQ subunit of the $TCNQ^{-}$–$TCNQ^{-}$ dianion, as well as the direction angles of the vector C 22–C 22′, which describes the long sigma bond in the dianion.

The conductivity of $(NEP^{+})_2(TCNQ^{-}\text{–}TCNQ^{-})$ at room-temperature, measured by the four-probe method on a single crystal, is of the order of $10^{-11}\ \Omega^{-1}\ cm^{-1}$.

### 2.2 Intense TSE spectrum

$S = 1$ signals were observed[13] in the temperature range $190 < T < 420$ K, and their temperature dependence could be fit to the empirical equation:

$$I(T) = I(0)\exp(-E_1/kT)$$

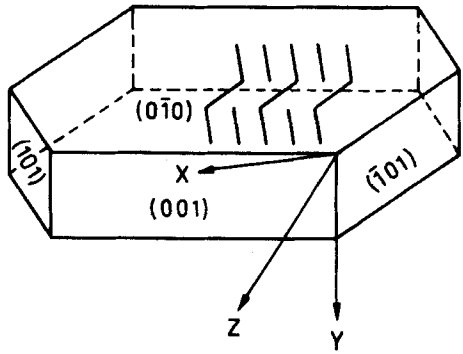


FIGURE 2 Habit of $(NEP^+)_2(TCNQ^-\text{-}TCNQ^-)$ crystals used for EPR studies, and definition of cartesian coordinates ($X$, $Y$, $Z$). For clarity the $TCNQ^-\text{-}TCNQ^-$ dianion orientation in the samples as inferred by X-ray analysis and from Ref. 8, is also shown schematically.

with $E_1 = 0.27 \pm 0.01$ eV (measured in the range $190 < T < 370$). In rough agreement with this fit, the triplet spin concentration in the sample at room temperature (measured by comparison with a sample of TEMPOL (4-Hydroxy-2,2,6,6-tetramethylpiperidine-1-oxyl (Lancaster Synthesis Ltd., England) and ruby (NBS)) was found to be $2.0 \pm 0.5 \times 10^{-3}$ spins/formula unit. The $S = 1$ signals are related below to excitations that "break" the long $\sigma$-bond in the $TCNQ^-\text{-}TCNQ^-$ dianion. Then $E_1$ is a measure of the thermal activation of this bond.

The fine-structure Hamiltonian for any triplet ($S = 1$) state is given by:[14]

$$\hat{\mathscr{H}} = D(\hat{S}_z^2 - 2/3) + E(\hat{S}_x^2 - \hat{S}_y^2) \quad (1a)$$

$$= -F_{xx}\hat{S}_x^2 - F_{yy}\hat{S}_y^2 - F_{zz}\hat{S}_z^2 \quad (1b)$$

where $D$ and $E$ are unique parameters, $(x, y, z)$ is the principal axis coordinate system, and $-F_{xx}$, $-F_{yy}$ and $-F_{zz}$ are the eigenvalues of the traceless tensor. The fine structure splittings in Figure 3 were obtained in orthogonal crystal planes. The data were fit by a highfield approximation to Eq. 1, since $D$ and $E$ are small compared to $g\mu_B B_0$ at $B_0 \sim 0.3T$ ($X$-band) for organic radicals. The experimental values of $D$ and $E$ at 300 K are $D = \pm 0.0104(3)$ cm$^{-1}$ and $E = \mp 0.0014(6)$ cm$^{-1}$. The calculated values in Figure 3 are $D = 0.0102$ cm$^{-1}$, $E = 0.0014$ cm$^{-1}$ for principal axes $x, y, z$ oriented as shown in Figure 1.

EPR spectra are shown in Figure 4 along the three principal-axis orientations of the fine structure tensor at room temperature. Evident are also the $S = 1/2$ "impurity" signal, and the thermally activated narrow $S = 1/2$ signal (Figure 4c), which are discussed in the next sections. The less intense TSE signals cannot be observed under these conditions.

The temperature dependence of the fine structure parameter $D$ has also been determined. The parameter $D_{/\!/c}$ decreases gradually from 0.0107 cm$^{-1}$

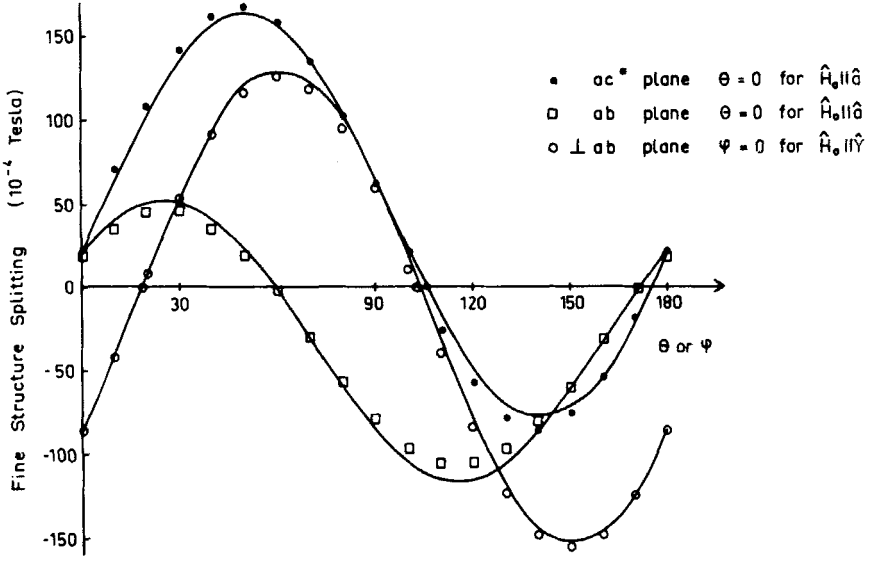


FIGURE 3 Comparison of the experimental and theoretical fine-structure splittings for the strong TSE lines in orthogonal crystal planes.

at 240 K to 0.0094 $cm^{-1}$ at 407 K. If the crystal is warmed up to 420 K, however, there is a rapid decrease of the fine structure splitting until only one broad featureless line is observed at 420 K. Upon cooling, the fine structure spectrum reappears reversibly. This collapse of the exciton lines is commonly observed in other $\pi$-$\pi$ overlapping triplet TCNQ salts, and also in [bis(2,2′-dipyridyl)Pt(II)]$^{2+}$(TCNQ$^-$–TCNQ$^-$), where a sharp phase transition occurs,[7] but in (NEP$^+$)$_2$(TCNQ$^-$–TCNQ$^-$) it occurs over a narrow temperature range from 410 to 420 K. This cannot be singly due to the temperature dependence of the triplet-exciton concentration.

The orientation of the experimental $F_{zz}$ is fairly close to the orientation of the C22–C22′ vector, while $F_{yy}$ is precisely along the projection of the $\sigma$-bond on the [100] plane in Figure 1b. What has clearly happened is that the triplet state forms, breaks the long sigma bond, and the spin densities rearrange so that the maximum spin densities shift away from the C22 and C$^{22'}$ atoms. The $F_{zz}$ orientation, instead of lying exactly along the C22–C22′ bond, moves towards a direction that points from one TCNQ ring to the other. There is probably some rehybridization of the sp$^3$ C22 and C22′ atoms.

In order to explain the magnitude and orientation of $D$ and $E$, a theoretical calculation[16] of the fine-structure parameters was carried out. To the extent

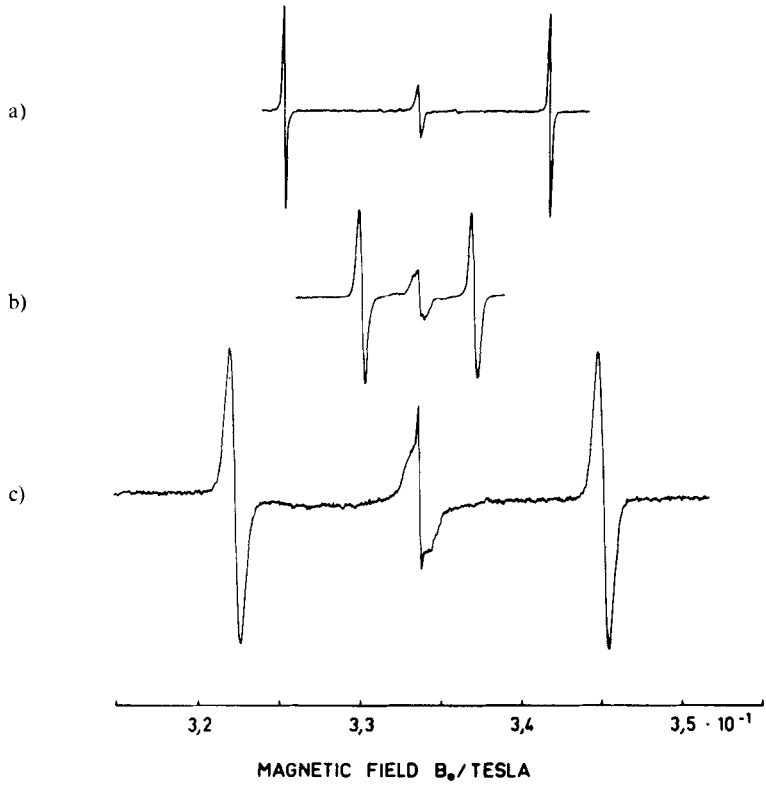


FIGURE 4 Fine-structure splittings along the principal axis directions $x$, $y$, $z$ whose orientation relative to the ($X$, $Y$, $Z$) cartesian system of Figure 2 is given in the last column of Table II. In Figures 4b, 4c, the "narrow" $S = 1/2$ signal can be seen in addition to the impurity signal.

that we are dealing with non-interacting molecular units, the dipole–dipole interaction $\hat{\mathscr{H}}_d$, if due to ion radicals A and B of known geometry, can be described by a 3 × 3 matrix,[17]

$$F_{pq} = \tfrac{1}{2} g^2 \mu_B^2 \sum_{\substack{i \in A \\ i \in B}} \rho_i \rho_j (r_{ij}^2 - 3 p_{ij} q_{ij}) r_{ij}^{-5} \qquad (2)$$

where $p, q = x, y, z$, and the ions are described by a set of spin densities $\rho_i$, $\rho_j$, localized at atom positions (atoms $i$ in radical $A$, atoms $j$ in radical $B$) with interatomic distances $r_{ij} = (x_{ij}^2 + y_{ij}^2 + z_{ij}^2)^{1/2}$. The eigenvalues of $F_{pq}$ are the $-F_{xx}$, $-F_{yy}$, $-F_{zz}$ of Eq. (1b). From these the theoretical estimates of $D = (1/2)(F_{xx} + F_{yy}) - F_{zz}$ and $E = -(1/2)(F_{xx} - F_{yy})$ can be obtained. The approximation of point spin densities in Eq. (2) must eventually fail at

TABLE II

Eigenvalues $F_{xx}$, $F_{yy}$, and $F_{zz}$ ($cm^{-1}$) and directional angles of eigenvectors (degrees) relative to the cartesian coordinate system of Figure 2 from experiment (at 300 K) and for four theoretical calculations (Eq. 2) of the $TCNQ^-$-$TCNQ^-$ $S = 1$ dianion using atom positions from Ref. 8 and the spin densities of Table III. In column (d) the spin densities of Table III (c) were used, but the spin densities of atoms C22 and C23, N27 and N30, etc. were interchanged

| | Experiment | | (a) | | (b) | | (c) | | (d) | |
|---|---|---|---|---|---|---|---|---|---|---|
| $F_{xx}$ | ± 0.00487(6) | 80° | 0.01207 | 79° | 0.01201 | 79° | 0.02945 | 80° | 0.00566 | 79° |
| | | 31° | | 34° | | 33° | | 33° | | 34° |
| | | 119° | | 121° | | 121° | | 121° | | 122° |
| $F_{yy}$ | ± 0.00207(6) | 39° | 0.00846 | 39° | 0.00899 | 42° | 0.02579 | 48° | 0.00349 | 35° |
| | | 115° | | 117° | | 118° | | 120° | | 115° |
| | | 118° | | 116° | | 119° | | 124° | | 113° |
| $F_{zz}$ | ∓ 0.00693(6) | 53° | −0.02035 | 43° | −0.02100 | 49° | −0.05524 | 44° | −0.00915 | 57° |
| | | 73° | | 71° | | 73° | | 77° | | 69° |
| | | 42° | | 54° | | 45° | | 50° | | 41° |

small separations, where the spatial extent of the atomic orbitals must be considered.

The crystal structure yields the ground state, or singlet, geometry which presumably relaxes on breaking the long $\sigma$-bond. The results in Table II support this conclusion, that the singlet geometry overestimates $D$ and $E$ for the TSE. Three different sets of theoretical spin densities were used (Table III) for the $TCNQ^-$–$TCNQ^-$ diradical. One (a) is a minimum-basis set *ab initio* calculation for $TCNQ^-$ with $D_{2h}$ symmetry, as used for $D$ and $E$ values in RbTCNQ(I).[17a,18] The next two sets involve open-shell INDO calculations:[16] set (b) is obtained for the $TCNQ^-$ ion in RbTCNQ(I) ($C_1$ symmetry); the spin densities were $D_{2h}$ symmetrized before use on $TCNQ^-$–$TCNQ^-$. The last set (c) is from an INDO calculation on the $TCNQ^-$ ion, with atomic coordinates from the $(NEP^+)_2(TCNQ^-$–$TCNQ^-)$ crystal structure (that is, the distorted "half" of the dianion). All spin densities are rather close, but, as expected, for set (c), the spin density at C22, the $sp^3$ carbon participating in the long sigma bond, is much larger than in the more conventional $TCNQ^-$ geometries. The calculated fine-structure parameters $F_{xx}$, $F_{yy}$, and $F_{zz}$, with their orientation relative to the cartesian coordinate system of Figure 2, are compared with experiment in Table II. There is *close agreement in orientation* of the theoretical and experimental fine structure tensors, but *strong disagreement in the magnitudes* of the principal values. The large spin densities at C22 and C22′ are just too close together. The strong $r^{-3}$ dependence in Eq. (2) indicates that even a modest lengthening on breaking the bond would significantly reduce $F_{xx}$, $F_{yy}$, and $F_{zz}$ without greatly affecting the principal axes of the dimer.

TABLE III

Spin densities for the $TCNQ^-$ atoms in the $TCNQ^-$–$TCNQ^-$ dianion

| Atom name (from Ref. 8) | (a) Ab initio on $D_{2h}$ $TCNQ^-$ (from Ref. 18) | (b) INDO on $TCNQ^-$ | (c) INDO on $TCNQ^-$ in $(NEP^+)_2(TCNQ^-$-$TCNQ^-)$ |
|---|---|---|---|
| N25 | 0.039 | 0.05908 | 0.0376 |
| N27 | 0.039 | 0.05908 | 0.0356 |
| N28 | 0.039 | 0.05908 | 0.0640 |
| N30 | 0.039 | 0.05908 | 0.0620 |
| C15 | 0.109 | 0.07309 | 0.0618 |
| C16 | 0.059 | 0.05196 | 0.0531 |
| C17 | 0.059 | 0.05196 | 0.0512 |
| C18 | 0.059 | 0.05196 | 0.0351 |
| C19 | 0.059 | 0.05196 | 0.0331 |
| C20 | 0.109 | 0.07309 | 0.0715 |
| C22 | 0.191 | 0.20147 | 0.3491 |
| C23 | 0.191 | 0.20147 | 0.1226 |
| C21 | 0.002 | 0.00167 | 0.0076 |
| C24 | 0.002 | 0.00167 | 0.0015 |
| C26 | 0.002 | 0.00167 | 0.0013 |
| C29 | 0.002 | 0.00167 | 0.0085 |

A different method of separating the spin densities in the triplet state was assumed for column *d* in Table II. Instead of changing the separation, the spin densities are "reorganized" so that the largest densities are at the ends of the $TCNQ^-$–$TCNQ^-$ dimer. The spin densities of Table IIIc were switched end for end, by interchanging C22 with C23, N27 with N30, etc. The principal axes remain in satisfactory agreement, while the magnitudes are far more satisfactory. Until the geometry of the "relaxed" $TCNQ^-$–$TCNQ^-$ triplet is accurately known, there can be no quantitative computation of $F_{xx}$, $F_{yy}$, and $F_{zz}$ in Eq. 1. The identification of the strong TSE signal with the $TCNQ^-$–$TCNQ^-$ dimer, on the other hand, is clear from the principal axes needed for the fit in Figure 3.

The TSE linewidths are shown in Figures 5 and 6 as function of orientation and temperature. No hyperfine structure is observed. The profiles are approximately Lorentzian. These lines are remarkably broad compared to other TSE salts.[3a] Furthermore, the strong correlation between linewidth and triplet-exciton density is not seen in Figure 6, since $\Delta B$ is weakly varying while $I(T)$ changes by orders of magnitude for $E_1 = 0.27$ eV.

At room temperature the TSE signals for $(NEP^+)_2(TCNQ^-$–$TCNQ^-)$ are *broadest* (0.74 mT, Figure 5b) when the magnetic field is in the principal *zy*-plane, about 30° from *z*, i.e. between the crystallographic *a*-axis and the normal to the $TCNQ^-$ molecular plane. The *narrowest* linewidth (0.11 mT)

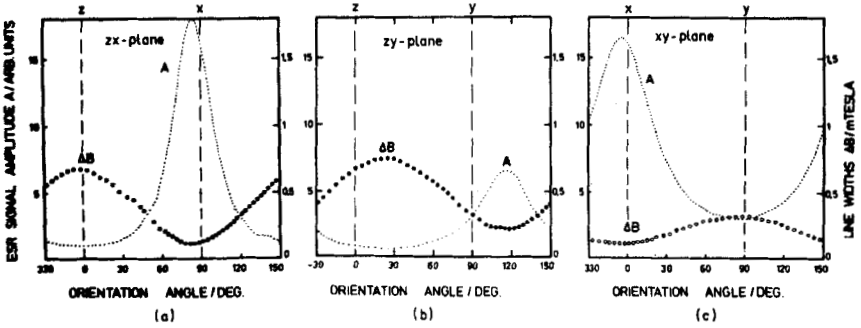


FIGURE 5 Orientation dependence of the linewidth (○○○○) (measured between points of maximum slope) and of the peak-to-peak amplitude of the first derivative (····) of the intense TSE fine structure lines in the *zx* (Figure 5a) principal axis plane, in the *zy* (Figure 5b) plane, and in the *xy* (Figure 5c) plane.

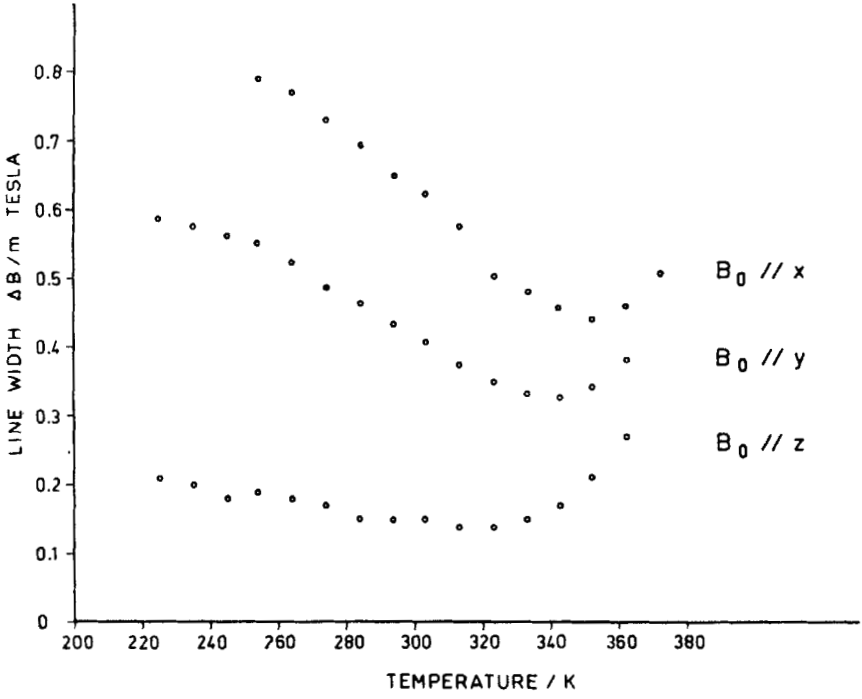


FIGURE 6 Temperature dependence of linewidth of the strong TSE signals with $B_0$ parallel to the principal axes *x*, *y*, *z*.

is observed in the $xy$-plane, about 6° from the $x$-direction (Figure 4a), i.e., the TSE lines are narrowest perpendicular to the stacking direction almost parallel to $b$. The isotropic (solution) hyperfine constant is only $a_H = 0.14$ mT[19] for each $TCNQ^-$ proton. Eight protons for a $TCNQ^-$–$TCNQ^-$ dimer, which no longer has $D_{2h}$ symmetry or equivalent protons, might possibly yield a partly resolved hyperfine pattern. The role of the nitrogen nuclei, the anisotropies of $a_H$, the deviations from planarity etc. would have to be considered. Recent computations[20] on cis$(CH)_x$, with a far larger $a_H$ of $\sim 3$ mT and a spin density spread over $\sim 15$ carbon atoms, yield a comparable linewidth of several 0.1 mT and illustrate the washing out of hyperfine structure for immobile but delocalized spins. The broad $(NEP^+)_2(TCNQ^-$–$TCNQ^-)$ lines certainly rule out the usual rapid TSE motion, but the present data does not distinguish between slow motion and complete immobilization. Additional relaxation mechanisms[21] involving exchange through $NEP^+$ or between $TCNQ^-$–$TCNQ^-$ dimers in different stacks can readily be postulated by analogy with other systems, but these processes are not well understood. Without attempting quantitative linewidth analysis, we merely characterize the TSE as "quasi-immobile" and not dominated by the usual relaxation mechanisms[21] involving exciton–exciton collisions.

### 2.3 The weak TSE signals

The fine-structure splittings of the less intense TSE signals are shown as larger circles in Figure 7, together with the intense TSE(· · ·). Their linewidths are comparable to those of the intense TSE signals. Additional weak signals have been observed[3b,22] in other TSE salts. They were tentatively associated[22] with misfit $TCNQ^-$ dimers from adjacent stacks. Since their activation energies are quite low, of the order of a few $cm^{-1}$, they are only significant

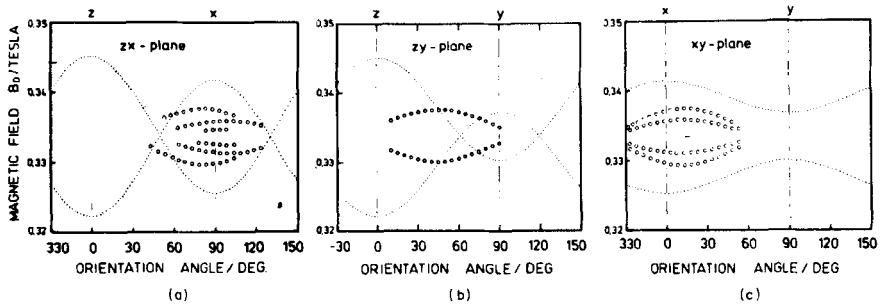


FIGURE 7 Orientation dependence of the intense (· · ·) and weak (○○○○) TSE fine-structure splittings in the $zx$ (Figure 7a) principal axis plane, in the $zy$ (Figure 7b) plane, and in the $xy$ (Figure 7c) plane.

at low temperatures relative to the strong TSE. The weak TSE in $(NEP^+)_2$ $(TCNQ^-–TCNQ^-)$ show smaller fine structure splittings and different principal axes than the strong ones (Figure 7) and a magnetic behaviour that roughly follows a Curie law down to 1.4 K. There are many candidates for additional paramagnetic centers: neutral NEP radicals via back charge-transfer, misfit $TCNQ^-$, higher spin states, etc. The present data does not allow us to draw precise conclusions.

## 3 THE $S = 1/2$ SPECTRA

### 3.1 The broad $S = 1/2$ "impurity signal"

As is common in all TSE salts, an exchange-narrowed $S = 1/2$ "impurity line" at $g$ close to the free electron value (2.00232) is observed. Its linewidth (Figure 4) at room temperature varies between 0.1–1.2 mT as the crystal is rotated. It may arise from the various domain boundary effects, lattice stacking errors, and other usual lattice defects that are unavoidable even after careful purification in organic ion-radical salts.

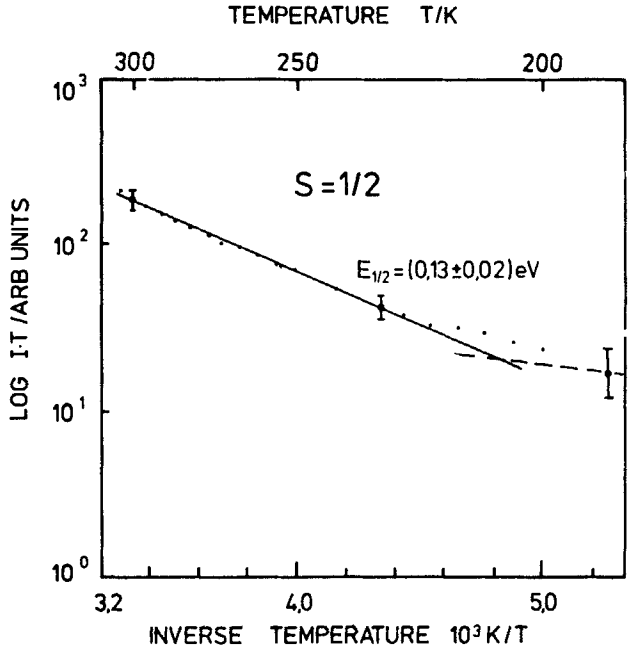


FIGURE 8 Arrhenius plot for the integrated EPR intensity $I$ as a function of absolute temperature $T$ for the "narrow" $S = 1/2$ EPR signal.

### 3.2 The "narrow" $S = 1/2$ signal

An additional thermally activated narrow signal is observable near $g = 2$ (Figure 4b, 4c) in a narrow angular range where it is not obscured by the broader impurity signal. Its temperature dependence is shown in Figure 8. In the temperature range of $220 < T < 300$ K the activation energy (expressed as $\log I(T) = A - E_{1/2}/kT$) is $E_{1/2} = 0.13(2)$ eV. Its linewidth at room temperature is about 0.05 mT. Since $2E_{1/2} \approx E_1$, these $S = 1/2$ species may be related to the strong TSE, but we do not have a specific model. This narrow, activated $S = 1/2$ resonance in $(NEP^+)_2(TCNQ^- - TCNQ^-)$ is quite different from the usual $g = 2$ features of TSE salts.

## 4 CONCLUSIONS

We have demonstrated a new type of TSE in a TCNQ-containing salt: Its thermally activated formation involves not the simple "spin flip" along a more or less regular linear chain of spin-paired $TCNQ^-$ anion radicals but the *breaking* of a rather long $\sigma$-bond (1.631 Å) that binds the two halves of the diamagnetic $TCNQ^- - TCNQ^-$ dianion in the ground state. This triplet state has an EPR linewidth about one order of magnitude greater than for previously studied TSE salts. Its roughly Lorentzian lineshape, lack of hyperfine structure, and orientation dependence suggest that it is "quasi-immobilized," in contrast to the usual, mobile TSE in organic ion-radical solids. Further work will show how general this behaviour may be in the system of *N*-alkylphenazinium-TCNQ and *N*-alkylphenazinium-$TCNQF_4$ salts.

## 5 Acknowledgment

One of us (R. M. Metzger) wishes to thank the Universität Heidelberg for a guest professorship. This work has been supported in part by Deutsche Forschungsgemeinschaft (Ke 135/21), Bonn-Bad Godesberg, Fonds der Chemischen Industrie, Frankfurt/M., Physikalisches Institut, Teil 3, Universität Stuttgart, and at Princeton University by NSF-DMR-7727418 AO1.

## References

1. D. S. Acker, R. J. Harder, W. R. Hertler, W. Mahler, L. R. Melby, R. E. Benson and W. E. Mochel, *J. Amer. Chem. Soc.*, **82**, 6408 (1960).
2. cf. reviews in (a) *Physics and Chemistry of Low-Dimensional Solids*, ed. L. Alcácer, Proceedings of NATO-ASI, Tomar, Portugal 1979, D. Reidel, Dordrecht, Holland, 1980. (b) *Molecular Metals*, ed. W. E. Hatfield, NATO-Conference Series VI: Materials Science Vol. 1, Plenum Press, New York, 1979. (c) *Quasi-One-Dimensional Conductors*, S. Barišic, A. Bjeliš, J. R. Cooper, and B. Leontic, ed., Lecture Notes in Physics, **95** and **96**, Springer, 1979. (d) *Low-Dimensional Cooperative Phenomena*, ed. H. J. Keller, NATO-ASI Series B,

Vol. 7, Plenum Press, New York, 1975. (e) *Chemistry and Physics of One-Dimensional Metals*, ed. H. J. Keller, NATA-ASI Series B, Vol. 25, Plenum Press, New York, 1977. (f) *Synthesis and Properties of Low-Dimensional Materials*, ed. J. S. Miller and A. J. Epstein, *Ann. N.Y. Acad. Sci.*, **313** (1978). (g) P. L. Nordio, Z. G. Soos and H. M. McConnell, *Ann. Revs. Phys. Chem.*, **17**, 237 (1966). (h) Z. G. Soos, *Ann. Revs. Phys. Chem.*, **25**, 121 (1974). Z. G. Soos and D. J. Klein, in *Molecular Association*, Vol. 1 (ed. R. Foster, Academic, New York, 1975), pp. 1–119.

3. (a) D. B. Chesnut and W. D. Phillips, *J. Chem. Phys.*, **35**, 1002 (1961). (b) D. B. Chesnut and P. Arthur, *J. Chem. Phys.*, **36**, 2969 (1962). (c) M. T. Jones and D. B. Chesnut, *J. Chem. Phys.*, **38**, 1311 (1963).
4. (a) D. D. Thomas, H. J. Keller, and H. M. McConnell, *J. Chem. Phys.*, **39**, 2321 (1963), ($TMPD^+ClO_4^-$). M. Inoue, H. Kuramoto and D. Nakamura, *Bull. Chem. Soc. Japan*, **50**, 2885 (1977), ($TMPD^+ClO_4^-$). (b) J. Yamauchi, H. Fujita and Y. Deguchi, *Bull. Chem. Soc. Japan*, **52**, 2819 (1979), ($TMPD^+BF_4^-$).
5. (a) R. H. Boyd and W. D. Phillips, *J. Chem. Phys.*, **43**, 2927 (1965). (b) R. Bozio, A. Girlando, and C. Pecile, *J. Chem. Soc. Faraday Trans. II*, **71**, 1237 (1975). (c) R. Bozio, I. Zanon, A. Girlando, and C. Pecile, *J. Chem. Soc. Faraday Trans. II*, **74**, 235 (1978). (d) T. Sakata, A. Nakane, and H. Tsubomura, *Bull. Chem. Soc. Japan*, **48**, 3391 (1975) report a peculiar dependence of the enthalpy of dimerization in water on the addition of ethanol or methanol: $\Delta H$ rises from −42 to −84 kJ/mole as the ethanol concentration rises from 0 % to 20 %.
6. Z. G. Soos, S. Mazumdar, and T. T. P. Cheung, *Mol. Cryst. Liq. Cryst.*, **52**, 93 (1979).
7. Vu Dong, H. Endres, H. J. Keller, W. Moroni, and D. Nöthe, *Acta Cryst.*, **B33**, 2428 (1977).
8. B. Morosin, H. J. Plastas, L. B. Coleman, and J. M. Stewart, *Acta Cryst.*, **B34**, 540 (1978).
9. H. B. Burgi and L. S. Bartell, *J. Amer. Chem. Soc.*, **94**, 5236 (1972).
10. W. Littke and U. Drück, *Angew. Chemie*, **91**, 434 (1979).
11. R. H. Harms, unpublished results.
12. A similar procedure has been described by L. R. Melby, *Can. J. Chem.*, **43**, 1448 (1965).
13. The EPR studies were performed on a Bruker B-ER 418 Spectrometer, Heidelberg and a Varian E-line Spectrometer, Stuttgart.
14. cf. e.g. A. Carrington and A. D. McLachlan, *Introduction to Magnetic Resonance*, Harper & Row, New York, 1967, pp. 116–121.
15. Z. G. Soos and D. J. Klein, in *Molecular Association*, ed. R. Foster, Academic Press, New York, 1975.
16. The calculations were carried out at the Universitätsrechenzentrum, Heidelberg, and on IBM 370/168 computer. Computer program CNINDO, based for the INDO calculations, is from QCPR II, 141, 1978. The fine structure program was checked by repeating the calculations of Ref. 17a and Ref. 17b.
17. (a) A. J. Silverstein and Z. G. Soos, *Chem. Phys. Letters*, **39**, 525 (1976). (b) C. P. Keijzers and D. Haarer, *J. Chem. Phys.*, **67**, 925, 1977. (c) S. Flandrois and J. Boissonade, *Chem. Phys. Letters*, **58**, 596 (1978).
18. H. T. Jonkman, G. van der Welde, and W. C. Niewpoort, *Chem. Phys. Letters.*, **25**, 62 (1974).
19. P. H. H. Fischer and C. A. McDowell, *J. Amer. Chem. Soc.*, **85**, 2694 (1963).
20. B. R. Weinberger, E. Ehrenfreund, A. Pron, A. J. Heeger, and A. G. McDiarmid, *J. Chem. Phys.*, **72**, 4749 (1980).
21. Z. G. Soos and H. M. McConnell, *J. Chem. Phys.*, **43**, 3780 (1965).
22. I. M. Brown and M. T. Jones, *J. Chem. Phys.*, **51**, 4687 (1969).

# MOLECULAR CRYSTALS